Quasi-biennial oscillation and quasi-biennial oscillation–annual beat in the tropical total column ozone: A two-dimensional model simulation

Xun Jiang
Division of Geological and Planetary Sciences, California Institute of Technology, Pasadena, California, USA

Department of Environmental Science and Engineering, California Institute of Technology, Pasadena, California, USA

Charles D. Camp
Department of Applied and Computational Mathematics, California Institute of Technology, Pasadena, California, USA

Runlie Shia, David Noone, Christopher Walker, and Yuk L. Yung
Division of Geological and Planetary Sciences, California Institute of Technology, Pasadena, California, USA

Received 24 November 2003; revised 24 March 2004; accepted 2 June 2004; published 20 August 2004.

[1] The National Centers for Environmental Prediction–Department of Energy Reanalysis 2 data are used to calculate the monthly mean meridional circulation and eddy diffusivity from 1979 to 2002 for use in the California Institute of Technology–Jet Propulsion Laboratory two-dimensional (2-D) chemistry and transport model (CTM). This allows for an investigation of the impact of dynamics on the interannual variability of the tropical total column ozone for all years for which the Total Ozone Mapping Spectrometer and the Solar Backscatter Ultraviolet merged total ozone data are available. The first two empirical orthogonal functions (EOFs) of the deseasonalized and detrended stratospheric stream function capture 88% of the total variance on interannual timescales. The first EOF, accounting for over 70% of the interannual variance, is related to the quasi-biennial oscillation (QBO) and its interaction with annual cycles, the QBO-annual beat (QBO-AB). The 2-D CTM provides realistic simulations of the seasonal and interannual variability of ozone in the tropics. The equatorial ozone anomaly from the model is close to that derived from the observations. The phase and amplitude of the QBO are well captured by the model. The magnitude of the QBO signal is somewhat larger in the model than it is in the data. The QBO-AB found in the simulated ozone agrees well with that in the observed data. *INDEX TERMS:* 0340 Atmospheric Composition and Structure: Middle atmosphere—composition and chemistry; 0341 Atmospheric Composition and Structure: Middle atmosphere—constituent transport and chemistry (3334); 3319 Meteorology and Atmospheric Dynamics: General circulation; 3334 Meteorology and Atmospheric Dynamics: Middle atmosphere dynamics (0341, 0342); 3362 Meteorology and Atmospheric Dynamics: Stratosphere/troposphere interactions; *KEYWORDS:* meridional circulation, Brewer-Dobson circulation, stratospheric ozone

Citation: Jiang, X., C. D. Camp, R. Shia, D. Noone, C. Walker, and Y. L. Yung (2004), Quasi-biennial oscillation and quasi-biennial oscillation–annual beat in the tropical total column ozone: A two-dimensional model simulation, *J. Geophys. Res.*, *109*, D16305, doi:10.1029/2003JD004377.

1. Introduction

[2] One of the major goals of upper atmosphere research is to observe the expected recovery of the ozone layer resulting from the regulation of chlorofluorcarbons (CFCs) and other ozone-depleting substances by the Montreal Protocol [*Austin et al.*, 2000; see also *World Meteorological Organization* (*WMO*), 2003, chap. 4]. Before the Montreal Protocol was implemented, the average rate of ozone depletion between 60°S and 60°N was ~2% per decade. The derivation of this loss rate was more reliable in the Southern Hemisphere (SH), where it was dominated by the occurrence of the Antarctic Ozone Hole in the austral spring. The signal was smaller in the Northern Hemisphere (NH) and subject to interference by a large seasonal cycle (5%) and an uncertain interannual variability (IAV) of ~2% [*WMO*, 2003, chap. 4]. Indeed, a substantial fraction of the observed ozone depletion may be attributed to the natural IAV in atmospheric dynamics [e.g., *Hood et al.*, 1997; *Fusco and Salby*, 1999; *Hadjinicolaou et al.*, 2002]. The question of what fraction of the change is chemical versus dynamical has never been satisfactorily resolved. The unambiguous detection of the expected recovery would be

0148-0227/04/2003JD004377$09.00

even more difficult because of the slow rate of decay of CFCs. *Stevermer and Weatherhead* [2001] estimated that it might take 15–35 years to detect this gradual recovery in the total column ozone, even under the best of circumstances. Therefore a better characterization of the IAV of ozone is urgently needed.

[3] *Shiotani* [1992] found quasi-biennial oscillation (QBO) and El Niño–Southern Oscillation (ENSO) signals in the total column ozone derived from the Total Ozone Mapping Spectrometer (TOMS) from 1979 to 1989. Using the Merged Ozone Data set (MOD), which combined the monthly mean column abundances collected by the TOMS and the Solar Backscatter Ultraviolet (SBUV and SBUV/2) instruments, *Camp et al.* [2003] carried out a principal component analysis (PCA) of the temporal and spatial patterns of the IAV of the total column ozone in the tropics from late 1979 to 2000 on a $5^\circ \times 10^\circ$ latitude-longitude grid. This study was a complete analysis of tropical ozone data using simultaneously the longitudinal, latitudinal, and temporal patterns. The first four empirical orthogonal functions (EOFs) of their study captured over 93% of the variance of the detrended and deseasonalized data on interannual timescales. The leading two EOFs, accounting for 42% and 33% of the variance, respectively, displayed structures attributable to the QBO, with influence from a decadal oscillation (most likely the solar cycle). The third EOF (15% of the variance) represented an interaction between the QBO and an annual cycle. The fourth EOF (3% of the variance) was related to the ENSO. In this paper, we will concentrate on the modeling of the QBO and the QBO-annual beat (QBO-AB), which together account for more than 50% of the IAV of tropical ozone. Other interannual variability, e.g., ENSO, will be studied in the future.

[4] The mechanism by which the QBO modulates ozone column abundance in the stratosphere is well known [*Plumb and Bell*, 1982; see also *Baldwin et al.*, 2001]. When the QBO is in the westerly (easterly) phase, there is descending (upwelling) anomalous motion in the tropical stratosphere and upwelling (descending) anomalous motion in the subtropical stratosphere. This results in more (less) ozone at the equator in the westerly (easterly) QBO phase [*Tung and Yang*, 1994a; *Randel and Cobb*, 1994]. The QBO period varies from about 22 to 32 months, with an average of 28 months. The interaction of the annual cycle with the QBO will produce two cycles with periods of approximately 20 and 8.6 months [*Tung and Yang*, 1994a]. These periods were first found in the total column ozone data obtained by TOMS in the tropics and extratropics [*Tung and Yang*, 1994a, 1994b].

[5] Several idealized numerical models have been developed to study the influence of the QBO on the ozone. Using a mechanistic model, *Hasebe* [1994] found that the phase of the ozone QBO approaches that of the temperature QBO. *Politowicz and Hitchman* [1997] introduced an analytic forcing of the stratospheric QBO in a two-dimensional (2-D) middle atmosphere model in three different ways. They used a different amplification factor for each method, seeking good agreement with the observed QBO in the column ozone, and found that the diabatic forcing method was better than that of wave driving and thermal nudging. Similarly, using an equatorial wave forcing parameterization, *Jones et al.* [1998] successfully generated a QBO with a period of ~28 months. The induced circulation in their model was stronger in the winter hemisphere. Further analysis of the *Jones et al.* [1998] model (X. Jiang et al., manuscript in preparation, 2004) reveals the existence of a QBO-AB signal at about 20 months. However, the *Jones et al.* [1998] model is an idealized model and it cannot simulate the IAV of the observed ozone.

[6] *Kinnersley and Tung* [1999] used an interactive stratospheric model by relaxing the equatorial zonal wind to the observed Singapore zonal wind. Their model simulates the observed ozone anomaly satisfactorily. However, there appears to be some underestimation of the equatorial QBO amplitude in the ozone column.

[7] *Fleming et al.* [2002] used the meteorological data from the United Kingdom Meteorological Office (UKMO) model and constituent data from the Upper Atmosphere Research Satellite (UARS) to calculate yearly zonal mean dynamical fields to drive the NASA Goddard Space Flight Center (GSFC) 2-D chemistry and transport model. This study provides a good simulation of the IAV of the total column ozone from 1993 to 2000. However, it underestimates the QBO amplitudes at the equator, partially because the UKMO temperatures underestimate the QBO amplitude by at least 40% [*Randel et al.*, 1999]. To compensate, *Fleming et al.* [2002] also calculated the total column ozone by increasing the QBO amplitude in the UKMO temperatures by 40%; however, their result still underestimates the QBO signal in MOD by nearly a factor of 2.

[8] *Pawson and Fiorino* [1998a, 1998b] studied the annual cycle and the QBO in the National Centers for Environmental Prediction–National Center for Atmospheric Research (NCEP-NCAR) Reanalysis 1 (NCEP1) and European Centre for Medium-Range Weather Forecasts (ECMWF) Reanalysis (ERA). They found high correlations between the zonal winds of both reanalyses and the observations. The northward velocities in the NCEP1 data showed a more realistic structure than those in the ERA data. *Randel et al.* [2000] found that the signatures of the QBO and ENSO events were strong in tropopause statistics from NCEP1 from 1957 to 1997.

[9] Using monthly mean meridional circulation to drive the California Institute of Technology–Jet Propulsion Laboratory (Caltech/JPL) 2-D chemistry and transport model (CTM), we carry out the first realistic simulation of the ozone QBO and QBO-AB from 1979 to 2002, coincident with the MOD record. The mean meridional circulation is derived from NCEP–Department of Energy Reanalysis 2 (NCEP2), provided by the National Oceanic and Atmospheric Administration (NOAA)–Cooperative Institute for Research in the Atmosphere (CIRES) Climate Diagnostics Center. We then apply PCA to the simulated ozone calculated by the 2-D CTM. The model ozone results for QBO and QBO-AB are compared to the signals obtained by *Camp et al.* [2003] from the MOD observations.

2. NCEP-Derived Transport Fields

2.1. Stream Function

[10] NCEP2 four-times-daily spectral coefficients are used to calculate the monthly mean meridional circulations from 1979 to 2002, using the method of *Johnson* [1989]. Recently, the same method was used by *Bartels et al.* [1998] to study

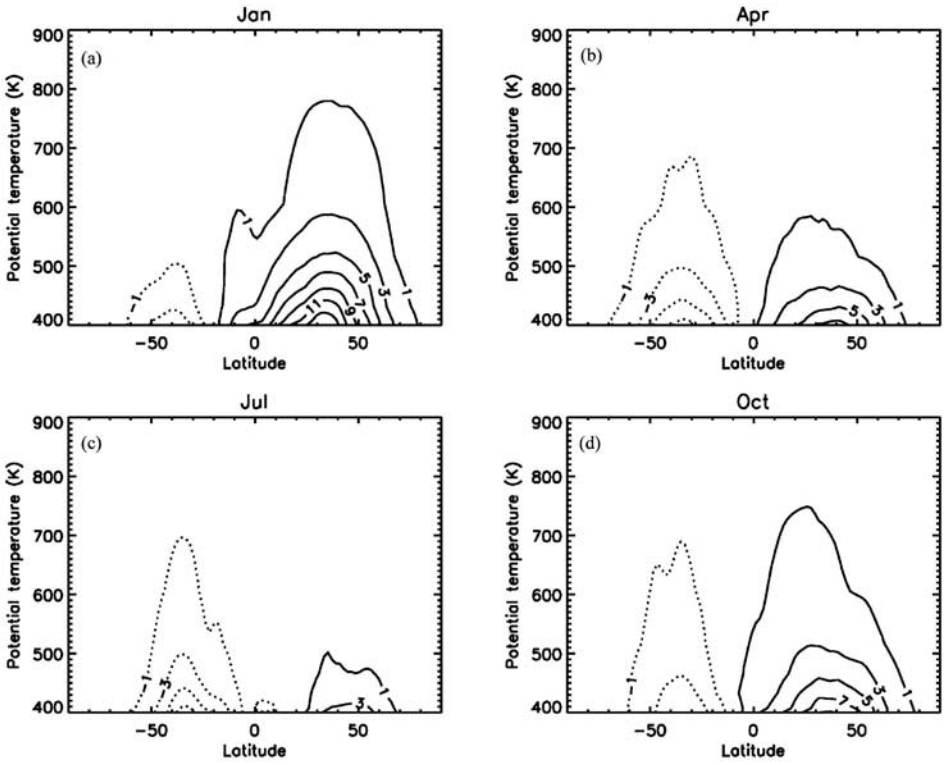

Figure 1. Stratospheric isentropic stream function in 1985. (a) January, (b) April, (c) July, and (d) October. Units are 10^9 kg/s.

the Ertel potential vorticity flux in the upper troposphere and lower stratosphere. *Held and Schneider* [1999] also applied this method to study the near-surface branch of the overturning mass transport circulation in the troposphere.

[11] The NCEP2 spectral coefficients are available on 28 sigma levels and with T62 (triangular wave number truncation at 62) resolution in the horizontal [*Kalnay et al.*, 1996; *Kistler et al.*, 2001]. On the pressure surface the 3-D meridional mass flux $\psi_P(\lambda, \varphi, p)$ is determined by

$$\psi_P(\lambda,\varphi,p) = \frac{2\pi a \cos\varphi}{g} \int_o^p V(\lambda,\varphi,p')dp', \qquad (1)$$

where a is the Earth radius; λ, φ, and p are the longitude, latitude, and pressure, respectively; V is the meridional velocity; and g is the gravitational acceleration rate. Then we interpolate the 3-D meridional mass flux to isentropic surfaces, using a mass-conserving linear interpolation scheme [*Juckes et al.*, 1994]. The 2-D isentropic mass stream function ψ_θ (φ, θ) is derived by zonal averaging of the 3-D isentropic meridional mass flux ψ_θ (λ, φ, θ) along isentropes. Finally, we interpolate the 2-D isentropic mass stream function ψ_θ (φ, θ) to pressure coordinates and scale by the density to produce the pressure surface stream function ψ_P (φ, p), which is used to drive the 2-D CTM.

[12] Figure 1 shows the 2-D isentropic mass stream function ψ_θ (φ, θ) in the stratosphere in January, April, July, and October of 1985. The air is drawn upward and poleward from the tropical lower stratosphere and pushed downward into the extratropical troposphere by the wave-induced forces [*Holton et al.*, 1995]. This circulation is important for the transportation of ozone and other trace species in the stratosphere. The seasonal variation is also captured well by this stream function. The stream function is strong in the NH in January, when the temperature gradient and wave activity are strong. As a result more ozone is transported to the northern polar region. The stream function becomes weaker in the spring and summer in the NH, when the temperature gradient and wave activity are weaker. Less ozone is transported to the northern polar region in these seasons. In the fall the stream function becomes strong again, and there is more poleward transport of ozone. The hemispheric asymmetry of the circulation verifies that the wave activity in the NH stratosphere is stronger than that in the SH.

[13] No previous results for the isentropic mass stream function in the stratosphere have been published, so we compare our results with the mass stream function computed in pressure coordinates shown in Figure 2 of *Shia et al.* [1989]. There is general agreement in the shape of these stream functions. The annual mean flux through the tropopause in the *Shia et al.* [1989] model is 9.3×10^9 kg/s, which is consistent with ^{14}C data. The analogous flux for our study is 14×10^9 kg/s. This is the flux through the 400-K isentropic surface, which is close to the tropical tropopause. These values demonstrate a reasonable agreement in the strength of the circulation from both studies.

[14] In previous studies the meridional circulation was usually computed from the net radiative heating rates using a diagnostic stream function model [see, e.g., *Ko et al.*, 1985]. However, these studies tended to exaggerate the tropical vertical transport through the tropopause. They therefore underestimated the total column ozone in the tropics and overestimated it in the extratropics [*Kinnersley and Tung*, 1999; *Fleming et al.*, 2002].

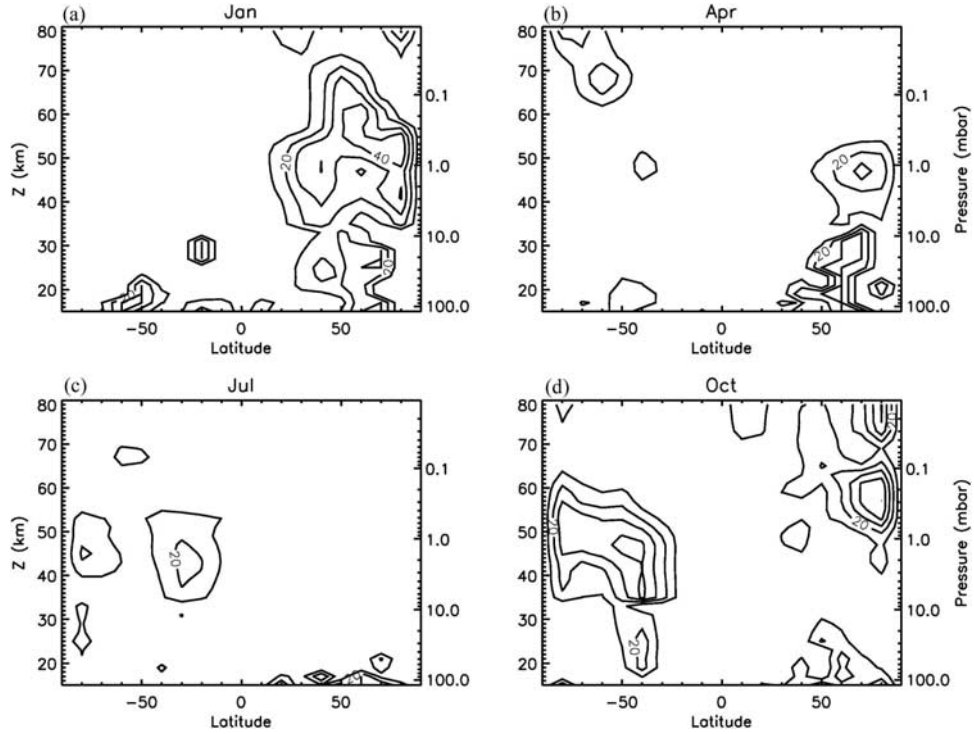

Figure 2. Isentropic mixing coefficient K_{yy} interpolated to the pressure surfaces in 1985. (a) January, (b) April, (c) July, and (d) October. Units are 10^5 m^2/s.

[15] Alternatively, the meridional circulation can also be represented by the direct transformed Eulerian-mean (TEM) circulation. This is hard to calculate accurately since there tends to be a strong cancellation between the eddy heat flux convergence and the adiabatic cooling; the diabatic heating term is the small residual of this cancellation [*Andrews et al.*, 1987]. The TEM circulation calculated from the residual velocity is shown in Figure A1[1] of the auxiliary material. This circulation displays counterrotating cells in the polar stratosphere that will cause unphysical transport of ozone. This may be due to the strong cancellation mentioned above or the poor quality of the meridional wind data in the polar stratosphere. In our model, we adopt the computed isentropic stream function, which is a closer approximation to the Lagrangian motion than is the residual mean meridional circulation.

2.2. Isentropic Mixing Coefficient K_{yy}

[16] In the lower stratosphere, zonal mean transport mainly takes the form of advection by the mean diabatic circulation in the meridional plane and eddy mixing approximately along isentropic surfaces [*Mahlman et al.*, 1984; *Tung*, 1984]. The isentropic mixing coefficient K_{yy} can be related to the Eliassen-Palm flux divergence [*Tung*, 1986; *Yang et al.*, 1990]. We calculate K_{yy} in the stratosphere from 1979 to 2002 using NCEP2 data. It is defined by

$$K_{yy} = -\widehat{P^*V^*} \Big/ \left(\frac{\partial \hat{P}}{\partial y}\right), \tag{2}$$

where $P = (\zeta + f)/\sigma$ is the Ertel potential vorticity; ζ is the relative vorticity, f is the planetary vorticity, and $\sigma = -(1/g)(\partial p/\partial\theta)$ denotes the density in the isentropic coordinates, where p and θ are the pressure and potential temperature of the isentropic surfaces. V is the meridional velocity, and $y = a \sin\varphi$, where a is the Earth's radius and φ is the latitude. The overbar denotes a zonal average along isentropes, e.g., for an arbitrary field $h(\lambda)$,

$$\overline{h} = \frac{1}{2\pi}\int_0^{2\pi} h d\lambda.$$

The hat denotes a mass-weighted zonal average, $\hat{h} = \overline{\sigma h}/\overline{\sigma}$, and the asterisk denotes the deviation from the mass-weighted zonal average, $h^* = h - \hat{h}$.

[17] The K_{yy} values are interpolated from the isentropic surfaces to the pressure surfaces for use in the 2-D CTM. Figure 2 shows the K_{yy} field on the pressure surfaces in January, April, July, and October of 1985. For surfaces between 15 and 35 km the K_{yy} values are calculated from the NCEP2 data set. Above 35 km and below 15 km the values are from *Fleming et al.* [2002] and consist of a climatologically seasonal cycle with no IAV. The values are large in the midlatitudes, on the order of 10^6 m^2 s^{-1}, and small in the high latitudes and tropics, on the order of 10^5 m^2 s^{-1}. K_{yy} is larger in the NH than in the SH, as a result of more wave activity in the NH. There are some negative K_{yy} values calculated from the NCEP2 data set where $\partial\hat{P}/\partial y$ changes sign, caused either by noise in the data or by the possible existence of local baroclinic and barotropic instability [*Yang et al.*, 1990]. For this study, negative values of K_{yy} were set to zero to avoid the numerical instability.

3. IAV of the Stream Function

[18] In order to study the IAV of the pressure surface stream function used to drive the 2-D CTM, we define a

[1] Auxiliary material is available at ftp://ftp.agu.org/apend/jd/2003JD004377.

stream function anomaly in the following manner. First, the time series for each grid point is decomposed as

$$\psi_p(t) = A_p^0 + A_p^1 t + \psi_p^a(t) + \psi_p'(t), \quad (3)$$

where the first two terms, $A_p^0 + A_p^1 t$, constitute a linear trend determined by a least squares fit. The mean annual cycle $\psi_p^a(t)$ is determined by evaluating the mean value for each month independently. To isolate the IAV from higher-frequency oscillations, a spectral filter is applied to the anomaly $\psi_p'(t)$. The filter is constructed as the convolution of a step function with a Hanning window and chosen to obtain a full signal from periods above 15 months and no signal from periods below 12.5 months. PCA is then performed on the filtered stream function anomaly. The details of the methodology are explained by *Camp et al.* [2003]. The first three EOFs from this analysis, along with the associated principal component (PC) time series and their power spectral estimate, are shown in Figures 3 and 4. All spectral estimates are calculated by Welch's method, averaging three half-length segments with 50% overlap; a Welch window is applied to each segment prior to averaging [*Press et al.*, 1992]. These three EOFs account for 95% of the total variance of the filtered stream function anomaly. The correlations (lag = 0) and maximum cross correlations between the PCs of the stream function and the relevant indices are given in Table 1. The corresponding significance levels are also listed. The significance statistics for correlations were generated by a Monte Carlo method [*Press et al.*, 1992]. A distribution of correlations was generated by determining the correlations of 3000 isospectral surrogate time series with the relevant indices. This distribution was transformed into an approximately normal distribution by the Fisher transformation [*Devore*, 1982]. The significance level of the actual correlation within the normal distribution was then determined. A small numerical value of the significance level denotes a high statistical significance.

[19] The first EOF, Figure 3a, captures over 70% of the variance and represents an oscillation in the strength of Brewer-Dobson circulation caused by the QBO. During the westerly (easterly) phase of the QBO the Brewer-Dobson circulation is weakened (strengthened). The associated principal component time series, PC1, is plotted in Figure 4a against the inverted 30-mbar QBO index (the zonal average of the 30-mbar zonal wind at the equator computed from the NCEP2). The power spectral estimate of PC1, Figure 4b, shows the 28-month mean period characteristic of the QBO. PC1 leads the 30-mbar QBO index by four months (derived from the maximum cross-correlation position), which is consistent with the occurrence of the maximum of the stream function anomaly variation above the 30-mbar level, since the QBO is characterized by a downward propagation. A secondary 20-month-period oscillation is also evident. The modulation of the annual cycle of the Brewer-Dobson circulation by the QBO results in the creation of two oscillations with frequencies equal to the difference and sum of the source frequencies, i.e., at periods of 20 and 8.6 months [*Tung and Yang*, 1994a]. Only the 20-month signal is evident, since the spectral filtering destroys the signal from the higher frequency. Variations in QBO captured by the EOF

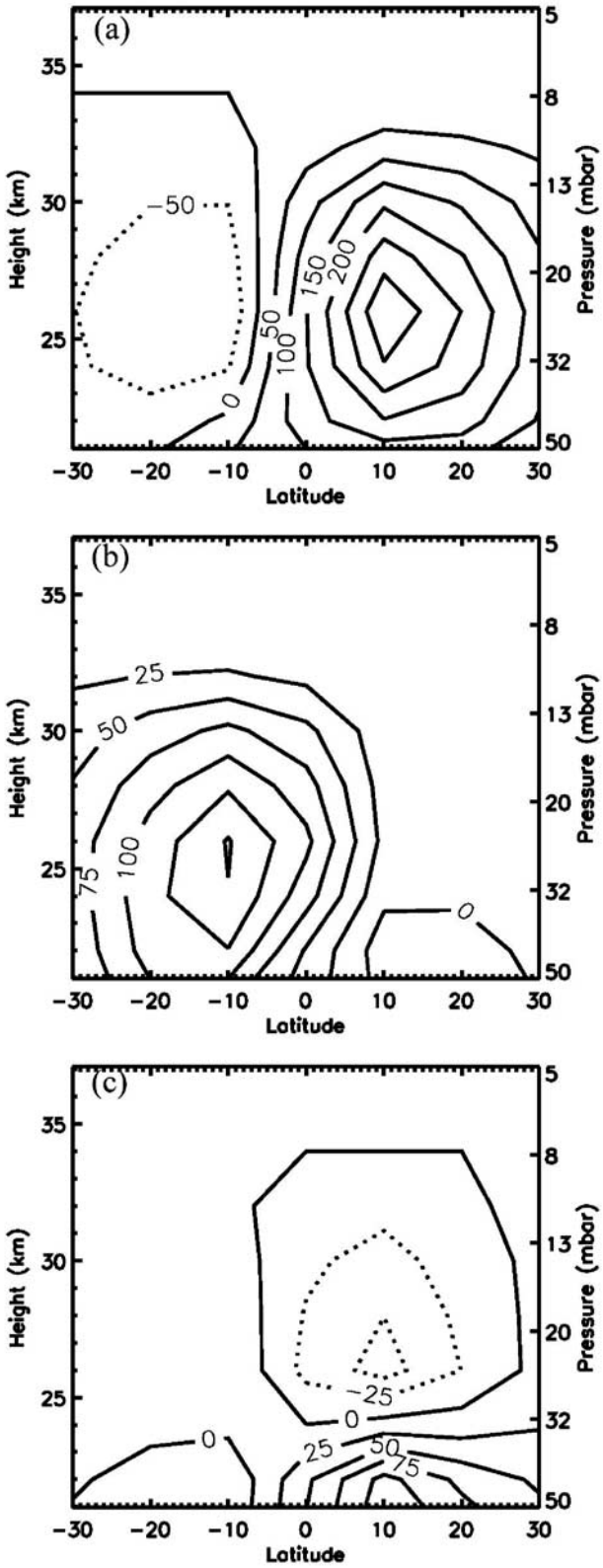

Figure 3. First three spatial EOF patterns of the pressure surface stream function. Units are m^2/s.

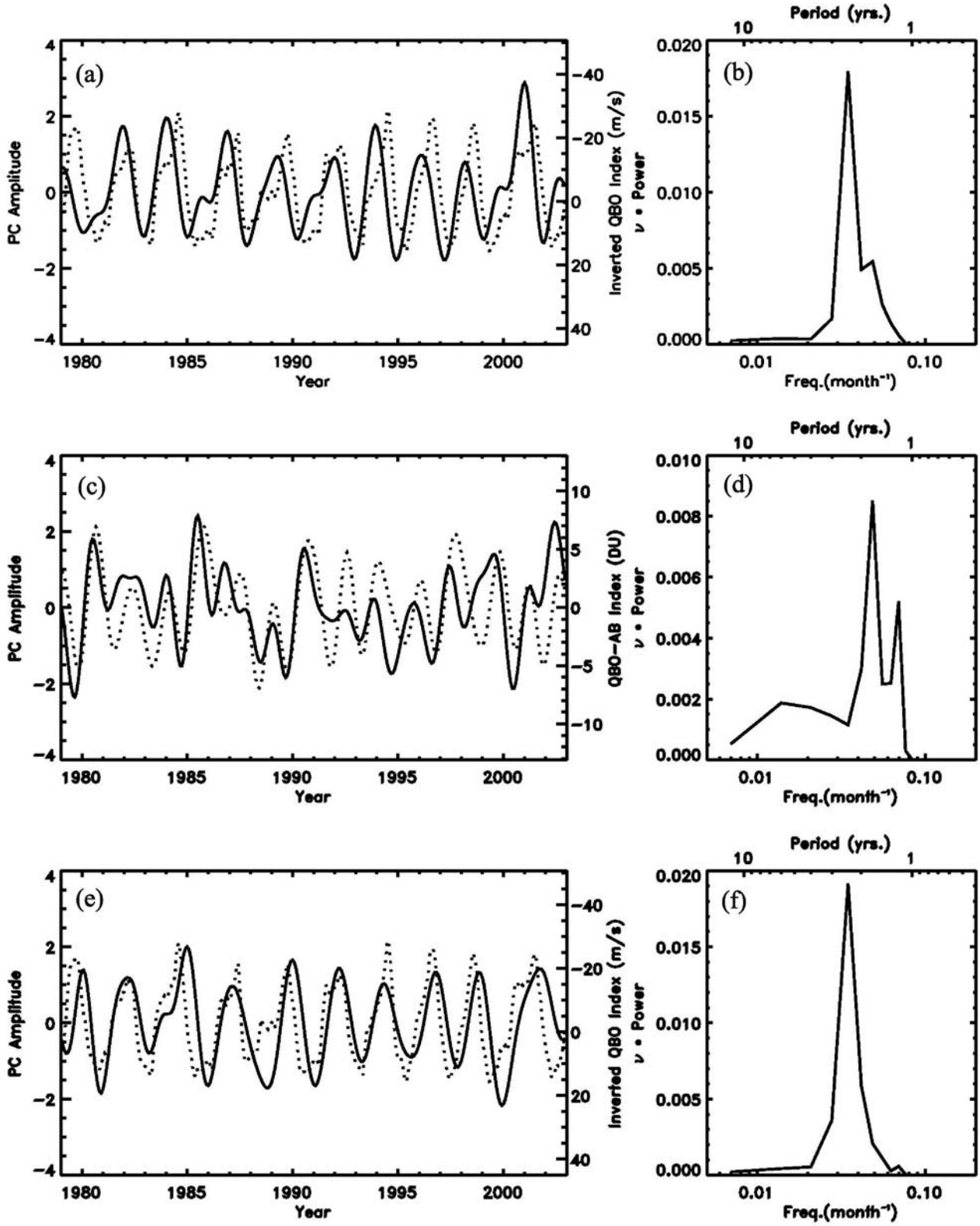

Figure 4. PC time series (left column) and spectra (right column) for the first three EOFs of the stream function. PCs (solid lines) are shown along with an appropriate index (dotted lines). PC1 and inverted 30-mbar QBO index (Figure 4a), PC2 and constructed QBO-AB index (PC3 of the zonal mean MOD) (Figure 4c), and PC3 and inverted 30-mbar QBO index (Figure 4e).

Table 1. Correlations (Lag = 0) and Maximum Cross Correlations of the Stream Function and Modeled Total Column Ozone PCs with Various Indices[a]

	QBO (30 mbar)	QBO-AB (PC3 of Zonal Mean MOD)	PC1 of Zonal Mean MOD
Stream function			
PC1	−0.46 (12.5%), lag = 0; −0.82 (0.4%), lag = 4		
PC2		0.52 (3.1%), lag = 0; 0.65 (0.4%), lag = 2	
PC3	−0.58 (7.3%), lag = 0; −0.81 (0.7%), lag = −3		
Modeled total column ozone			
PC1	0.87 (0.2%), lag = 0; 0.91 (0.1%), lag = 1		0.81 (0.3%), lag = 0; 0.86 (0.1%), lag = −1
PC2		0.50 (1.6%), lag = 0; 0.50 (1.6%), lag = 0	

[a]The numbers in parentheses denote significance levels. Units of lag are months. Positive (negative) lags correspond to the PC time series leading (trailing) the indices.

are distinctly asymmetric about the equator; the amplitude of variations of the northern lobe is greater than that of the southern by more than a factor of 3. This is the first time that an asymmetric QBO circulation has been found in the stream function derived from the NCEP2 data.

[20] The second EOF, Figure 3b, captures ~18% of the variance and represents a smaller variation in just the southern cell of the circulation. It oscillates with the 20-month period characteristic of the QBO-AB. The pattern of the 20-month signal is thus a linear combination of EOF1, containing the entire northern cell variability and some of the southern cell variability, and EOF2, containing the remaining southern variability. In Figure 4c, PC2 is shown against a constructed index for the QBO-AB (PC3 of the EOF results for the zonal mean MOD; see section 4 for details). PC2 correlates well with the QBO-AB (see Table 1).

[21] The third EOF, Figure 3c, captures ~6% of the variance and represents an oscillation in the height of the upwelling branch of the Hadley cell at the equator. Similar to PC1, the PC3 time series is dominated by a 28-month-period signal with a secondary 20-month-period signal. In Figure 4e, PC3 is shown along with the 30-mbar QBO index. PC3 lags the 30-mbar QBO index by 3 months,

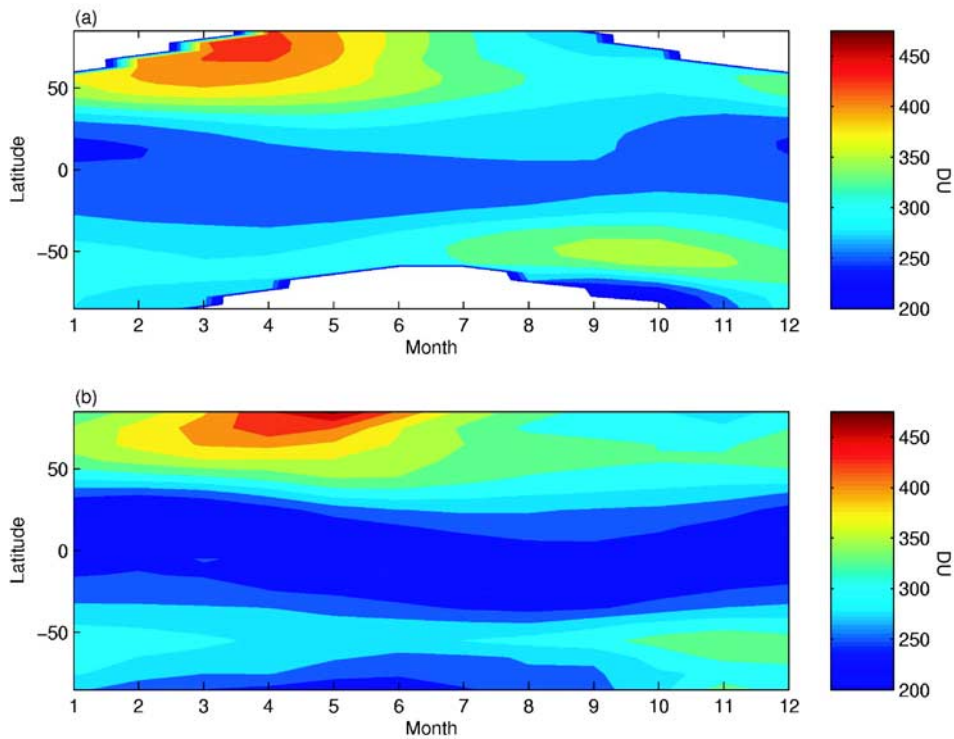

Figure 5. (a) The 1979–2002 mean of MOD and (b) 1979–2002 mean of total column ozone from 2-D model.

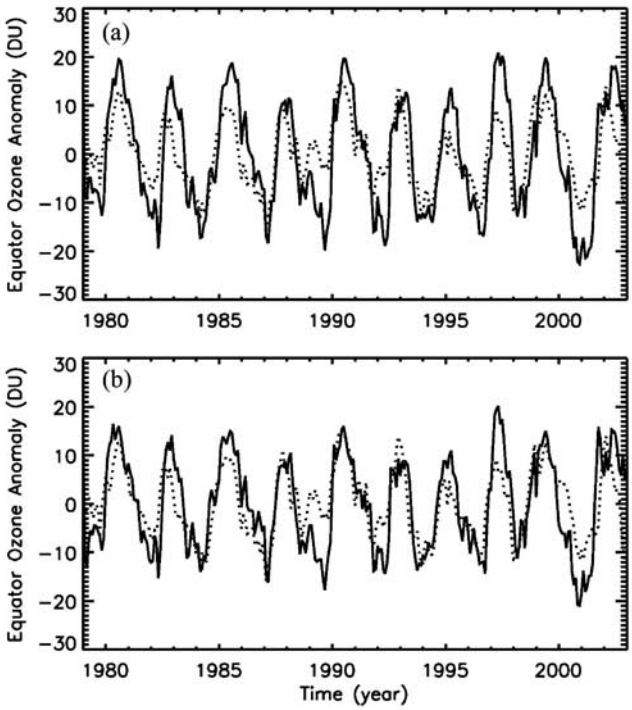

Figure 6. Equatorial detrended ozone anomaly from the 2-D Caltech/JPL CTM (solid lines), driven by (a) the original stream function and (b) the stream function in which the QBO component was reduced by a factor of 1.6. Both results are compared to the equatorial detrended ozone anomaly from MOD (dotted lines).

which is consistent with the occurrence of the center of the stream function anomaly variation below the 30-mbar level.

4. Modeling of Total Column Ozone in the Tropics

[22] The Caltech/JPL 2-D CTM is a zonally averaged model for trace species in the terrestrial troposphere and middle atmosphere (see *Shia et al.* [1989] and Appendix A of *Morgan et al.* [2004] for details). The model has 18 latitude boxes, equally spaced from pole to pole, and 40 layers, equally spaced in log (p) from the surface to the upper boundary at 0.01 mbar. Transport in the model is by the stream function and K_{yy} calculated from NCEP2 data sets. The values for K_{zz} are taken from *Summers et al.* [1997]. They are not important except in the mesosphere. The model includes all the gas-phase chemistry in the NASA recommendations for stratospheric modeling [*DeMore et al.*, 1997]. There is no heterogeneous chemistry. The numerical method used for solving the continuity equation in the model is the Prather scheme [*Prather*, 1986; *Shia et al.*, 1990].

[23] To understand the IAV of ozone, we model the total column ozone from 1975 to 2002. *Huesmann and Hitchman* [2001, 2003] and *Pawson and Fiorino* [1999] showed that there is a large discontinuity of the NCEP1 data when the TIROS Operational Vertical Sounder (TOVS) satellite data become available in 1979, so we use the first four years of data from NCEP1 only as spin-up time for the 2-D CTM. The stream function and eddy mixing coefficients from 1979 to 2002 are calculated from NCEP2. The climatology of total column ozone in these

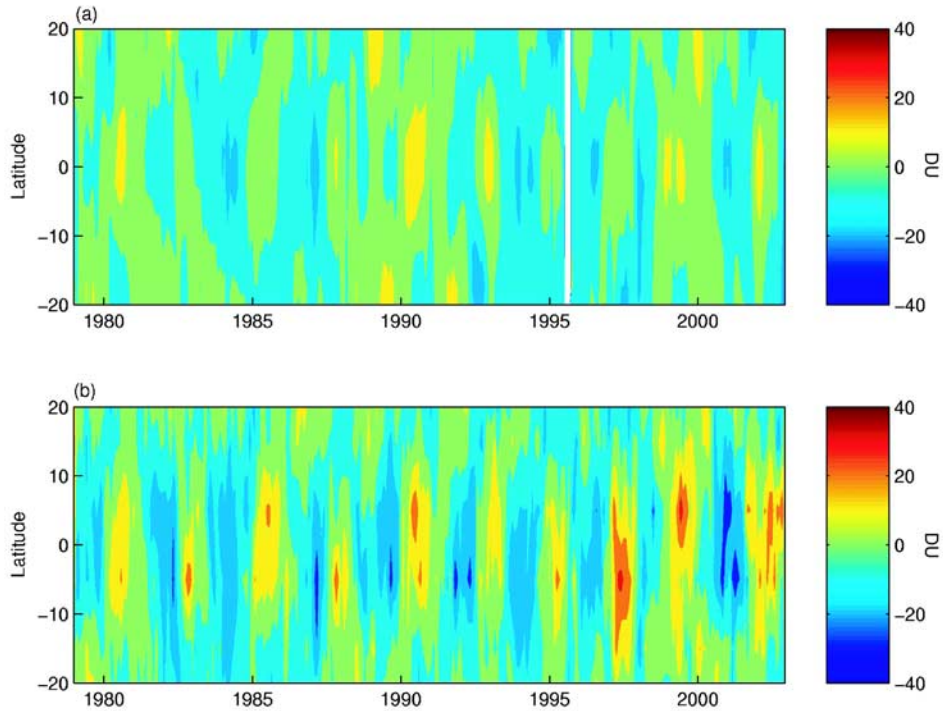

Figure 7. Latitude distribution of ozone anomaly from (a) MOD and (b) 2-D CTM driven by the original stream function.

24 years from the MOD [*McPeters et al.*, 1996] and the model results are compared in Figure 5. The model simulates the total column ozone well. In agreement with observations, more ozone is transported to the polar region by the stronger meridional circulation in the winter hemisphere than in the summer. Because the model does not incorporate heterogeneous chemistry, there are some differences in the high latitudes of the polar spring in both hemispheres. Furthermore, the strength of the SH stream function derived from NCEP2 is exaggerated; therefore the simulated total column ozone is lower than the MOD in the tropical summer. The NCEP2 meridional wind field may not be realistic in the high latitudes of the SH because there are relatively few radiosonde measurements. Correlation coefficients and confidence levels between monthly mean column ozone from MOD and the model over the period from 1979 to 2002 are shown in Figure A2 of the auxiliary material. The correlation coefficients are high in most areas and are significant.

[24] The ozone anomaly is calculated by removing the mean monthly seasonal cycle from the original total column ozone. Figure 6a presents model results (solid line) for the equatorial total column ozone anomaly from 1979 to 2002. The linear trend has been removed by a least squares fit. The model provides a good simulation of the MOD anomaly (dotted line). The correlation coefficient of these two curves is 0.75, and the corresponding significance level is 0.4%. *Fleming et al.* [2002] first successfully calculated the residual mean meridional stream function using data from the UKMO general circulation model and UARS observations. Their results for the total column ozone are a good simulation of the MOD from 1993 to 2000. However, their model underestimates the tropical total column ozone. In our model the tropical column ozone anomaly is somewhat larger than it is in the observed data.

[25] The ratio of the standard deviations between the model and MOD tropical ozone anomaly is 1.6. In a sensitivity study we therefore reduced the QBO part of the stream function by a factor of 1.6. The QBO component in the detrended stream function anomaly was calculated by a linear regression against the 30-mbar QBO index. Then we used the stream function with weakened QBO to drive our 2-D CTM. The result is shown in Figure 6b. The correlation coefficient between the model and MOD curves is 0.75 with a significance level of 0.3%. The detrended ozone anomaly from our model is now closer in amplitude to the observed anomaly, while preserving the good match in phase seen in the results derived from the original stream function.

[26] The latitudinal distribution of the total column ozone anomaly from 1979 to 2002 is plotted in Figure 7. The 2-D CTM (Figure 7b) reproduces the seasonal and IAV of the MOD (Figure 7a) well, although there is some overestimation of the amplitude of variations in the tropics. There is an obvious QBO signal in the ozone anomaly from the 2-D CTM at the equator, which begins to propagate to high latitude in the winter and spring seasons.

[27] PCA is applied to the detrended, deseasonalized, and filtered total column ozone anomaly from the 2-D CTM. The filter is chosen to obtain a full signal from periods above 15 months and no signal from periods below 12.5 months. The first two EOFs, shown in Figures 8 and 9, capture

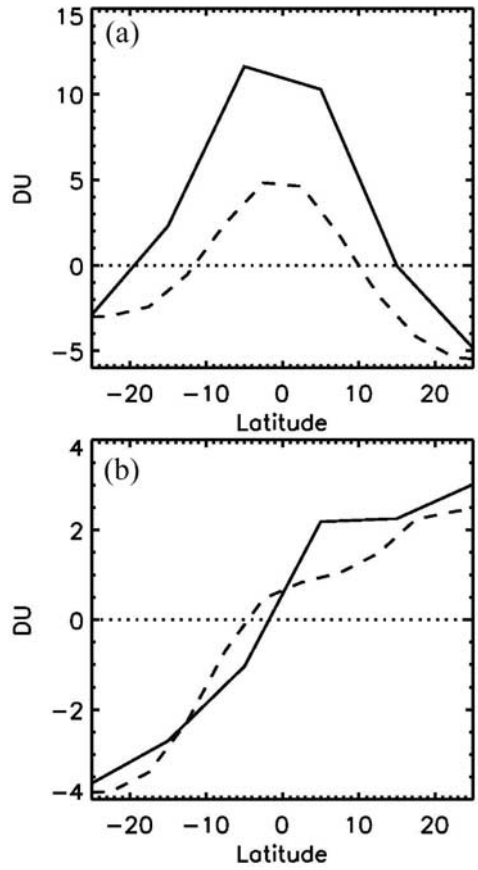

Figure 8. Spatial EOF patterns of the total column ozone. (a) First spatial EOF pattern of the total column ozone from 2-D CTM (solid line) and first spatial EOF pattern of the zonal mean MOD (dashed line). (b) Second spatial EOF pattern of the total column ozone from 2-D CTM (solid line) and third spatial EOF pattern of the zonal mean MOD (dashed line).

over 84% of the total variance of the filtered data. The first EOF, Figure 8a, captures 74% of the variance and displays a structure attributable to the QBO. It is asymmetric about the equator and oscillates about nodes at 15°N and 19°S. The values show a range from a high of 11.6 Dobson units (DU) to a low of −5 DU. The magnitude of this mode is larger than that of the first EOF pattern of the zonal mean MOD. The associated principal component time series, 2-D CTM PC1, is plotted in Figure 9a against the PC1 of the zonal mean MOD and the 30-mbar QBO index; it shows strong correlations with these indices (see Table 1). The power spectral estimate of PC1, Figure 9b, shows a strong peak at 28 months. The characteristics of this EOF are consistent with the modulation of the meridional circulation by the QBO as discussed in section 3.

[28] The second EOF, capturing 10.8% of the variance, is a tilted plane oscillating about a node at the equator (Figure 8b). Values range from 3 DU in the north to −3.5 DU in the south. It is similar to the third EOF pattern of the zonal mean MOD. In Figure 9c, 2-D CTM PC2 is shown against the PC3 of the zonal mean MOD. The correlation between these two time series is good (see Table 1). The power spectral estimate of the associated

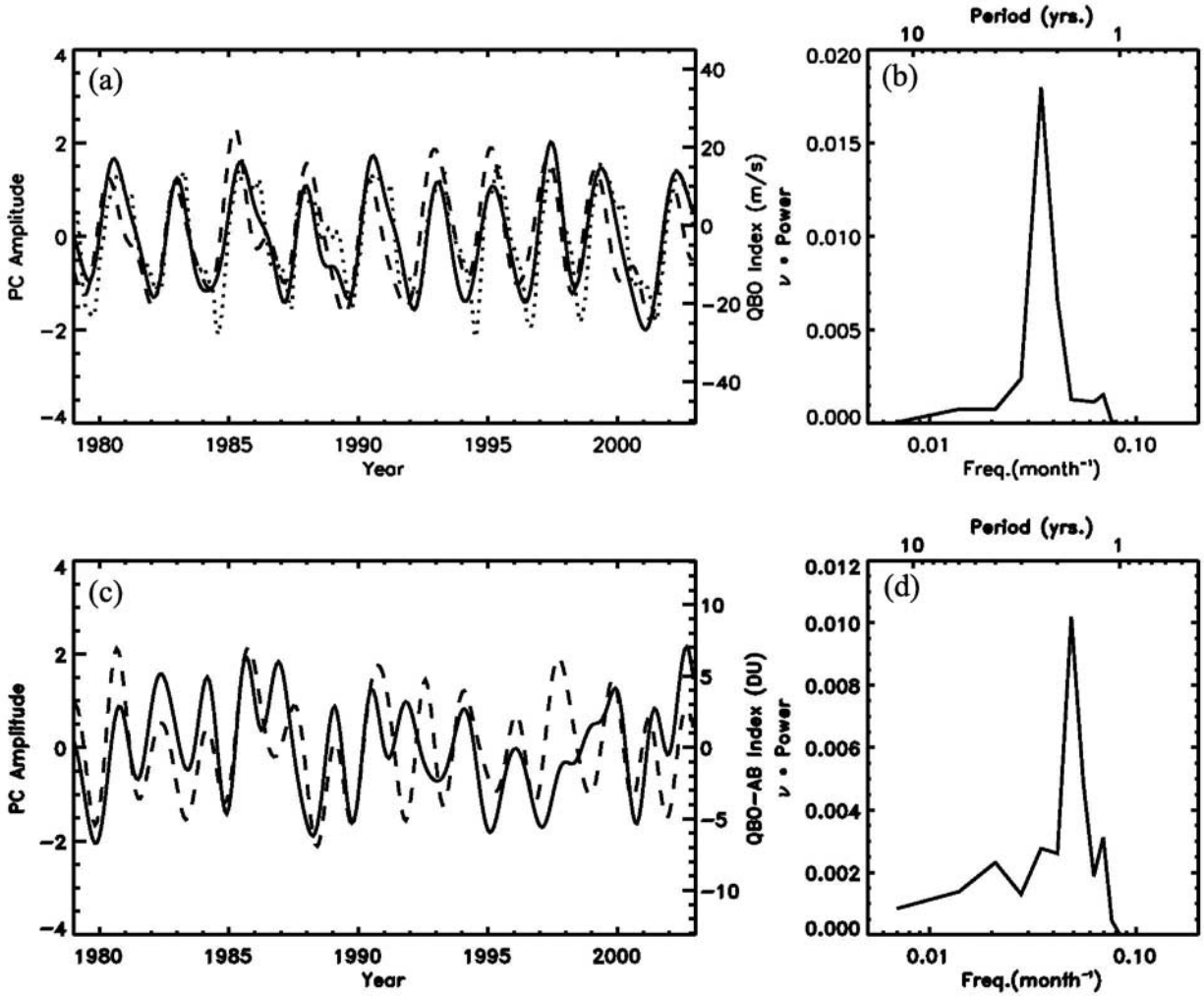

Figure 9. PC time series (left column) and spectra (right column) for the first two EOFs of the total column ozone from 2-D model. PCs are shown along with an appropriate index. (a) PC1 of the 2-D CTM ozone (solid line), PC1 of the zonal mean MOD (dashed line), and 30-mbar QBO index (dotted line) (Figure 9a). PC2 of the 2-D CTM ozone (solid line) and PC3 of the zonal mean MOD (dashed line) (Figure 9c).

PC2 has a dominant peak at 20 months, characteristic of the interaction between the QBO and annual cycles.

5. Conclusions

[29] We use a 2-D model to study the signals of QBO and QBO-AB in ozone. The NCEP2 dynamical fields are used to calculate the monthly mean meridional circulation on isentropic surfaces from 1979 to 2002. The isentropic stream function is then interpolated to pressure surfaces to drive the Caltech/JPL 2-D CTM. The 2-D CTM successfully simulates the seasonal and IAV of ozone in the tropics. The phase and amplitude of the QBO signal in the total column ozone in the tropics are captured by the model. The magnitude of the QBO signal is somewhat larger in the model than in the data. The model also simulates the QBO-AB well. The first two EOFs of the detrended, deseasonalized, and filtered total column ozone anomaly from the model capture over 84% of the total variance. The first EOF explains 74% of the variance and displays a structure attributable to the asymmetric QBO with a mean period of approximately 28 months. The second EOF, capturing 10.8% of the variance, is related to the approximately 20-month QBO-AB. All of these signals found in the model ozone are close to those in MOD. The successful simulation of the IAV of the total column ozone in the 2-D CTM suggests that the NCEP2 data have captured the bulk of IAV in the tropics.

[30] Since the 2-D meridional stream function cannot capture the longitudinal variation of the ENSO signal, no clear ENSO signal is found in the simulated total column ozone results. Future work will use a 3-D isentropic model to simulate the ENSO signal in the total column ozone. Similarly, since the decadal signal is only weakly present in our stream function, the simulated total column ozone does not show a decadal signal in the leading EOFs. Further work is also in progress to elucidate the detailed mechanism of the origin of QBO-AB and to extend these results to higher latitudes. In view of the obvious need to account for the natural IAV of ozone [see *Newchurch et*

al., 2003], it is important to extend this type of analysis to global ozone.

[31] **Acknowledgments.** We thank T. Schneider for kindly giving us his code for computing the stream function, E. Fleming for sending us his stream function, and K. K. Tung, V. Natraj, X. L. Huang, M. Gerstell, C. Parkinson, and two anonymous reviewers for helpful comments. This work was supported by NASA grant NAG1-1806.

References

Andrews, D. G., J. R. Holton, and C. B. Leovy (1987), *Middle Atmosphere Dynamics*, Academic, San Diego, Calif.

Austin, J., J. R. Knight, and N. Butchart (2000), Three-dimensional chemical model simulations of the ozone layer: 1979–2015, *Q. J. R. Meteorol. Soc.*, *126*, 1533–1556.

Baldwin, M. P., et al. (2001), The quasi-biennial oscillation, *Rev. Geophys.*, *39*, 179–229.

Bartels, J., D. Peters, and G. Schmitz (1998), Climatological Ertel's potential-vorticity flux and mean meridional circulation in the extratropical troposphere-lower stratosphere, *Ann. Geophys.*, *16*, 250–265.

Camp, C. D., M. S. Roulston, and Y. L. Yung (2003), Temporal and spatial patterns of the interannual variability of total ozone in the tropics, *J. Geophys. Res.*, *108*(D20), 4643, doi:10.1029/2001JD001504.

DeMore, W. B., et al. (1997), Chemical kinetics and photochemical data for use in stratospheric modeling: Evaluation 12, *JPL Publ.*, *97-4*.

Devore, J. L. (1982), *Probability and Statistics for Engineering and the Sciences*, 1st ed., 640 pp., Brooks/Cole, Monterey, Calif.

Fleming, E. L., C. H. Jackman, J. E. Rosenfield, and D. B. Considine (2002), Two-dimensional model simulations of the QBO in ozone and tracers in the tropical stratosphere, *J. Geophys. Res.*, *107*(D23), 4665, doi:10.1029/2001JD001146.

Fusco, A. C., and M. L. Salby (1999), Interannual variations of total ozone and their relationship to variations of planetary wave activity, *J. Clim.*, *12*, 1619–1629.

Hadjinicolaou, P., A. Jrrar, J. A. Pyle, and L. Bishop (2002), The dynamically-driven long-term trend in stratospheric ozone over northern mid-latitudes, *Q. J. R. Meteorol. Soc.*, *128*, 1393–1412.

Hasebe, F. (1994), Quasi-biennial oscillations of ozone and diabatic circulation in the equatorial stratosphere, *J. Atmos. Sci.*, *51*, 729–745.

Held, I. M., and T. Schneider (1999), The surface branch of the zonally averaged mass transport circulation in the troposphere, *J. Atmos. Sci.*, *56*, 1688–1697.

Holton, J. R., P. H. Haynes, M. E. McIntyre, A. R. Douglass, R. B. Rood, and L. Pfister (1995), Stratosphere-troposphere exchange, *Rev. Geophys.*, *33*, 403–439.

Hood, L. L., J. P. McCormack, and K. Labitzke (1997), An investigation of dynamical contributions to midlatitude ozone trends in winter, *J. Geophys. Res.*, *102*, 13,079–13,093.

Huesmann, A. S., and M. H. Hitchman (2001), The stratospheric quasi-biennial oscillation in the NCEP reanalyses: Climatological structures, *J. Geophys. Res.*, *106*, 11,859–11,874.

Huesmann, A. S., and M. H. Hitchman (2003), The 1978 shift in the NCEP reanalysis stratospheric quasi-biennial oscillation, *Geophys. Res. Lett.*, *30*(2), 1048, doi:10.1029/2002GL016323.

Johnson, D. R. (1989), The forcing and maintenance of global monsoonal circulations: An isentropic analysis, *Adv. Geophys.*, *31*, 43–316.

Jones, D. B. A., H. R. Schneider, and M. B. McElroy (1998), Effects of the quasibiennial oscillation on the zonally averaged transport of tracers, *J. Geophys. Res.*, *103*, 11,235–11,249.

Juckes, M. N., I. N. James, and M. Blackburn (1994), The influence of Antarctica on the momentum budget of the southern extratropics, *Q. J. R. Meteorol. Soc.*, *120*, 1017–1044.

Kalnay, E., et al. (1996), The NCEP/NCAR 40-year reanalysis project, *Bull. Am. Meteorol. Soc.*, *77*, 437–471.

Kinnersley, J. S., and K. K. Tung (1999), Mechanisms for the extratropical QBO in circulation and ozone, *J. Atmos. Sci.*, *56*, 1942–1962.

Kistler, R., et al. (2001), The NCEP-NCAR 50-year reanalysis: Monthly means CD-ROM and documentation, *Bull. Am. Meteorol. Soc.*, *82*, 247–267.

Ko, M. K. W., et al. (1985), A zonal mean model of stratospheric tracer transport in isentropic coordinates: Numerical simulations for nitrous oxide and nitric acid, *J. Geophys. Res.*, *90*, 2313–2329.

Mahlman, J. D., D. G. Andrews, D. L. Hartmann, T. Matsuno, and R. G. Murgatroyd (1984), Transport of trace constituents in the stratosphere, in *Dynamics of the Middle Atmosphere*, edited by J. R. Holton and T. Matsuno, pp. 387–416, Terra Sci., Tokyo.

McPeters, R., et al. (1996), Nimbus-7 Total Ozone Mapping Spectrometer (TOMS) data products user's guide, *NASA Ref. Publ.*, *1384*.

Morgan, C. G., M. Allen, M. C. Liang, R. L. Shia, G. A. Blake, and Y. L. Yung (2004), Isotopic fractionation of nitrous oxide in the stratosphere: Comparison between model and observations, *J. Geophys. Res.*, *109*, D04305, doi:10.1029/2003JD003402.

Newchurch, M. J., E.-S. Yang, D. M. Cunnold, G. C. Reinsel, J. M. Zawodny, and J. M. Russell III (2003), Evidence for slowdown in stratospheric ozone loss: First stage of ozone recovery, *J. Geophys. Res.*, *108*(D16), 4507, doi:10.1029/2003JD003471.

Pawson, S., and M. Fiorino (1998a), A comparison of reanalyses in the tropical stratosphere. Part 1: Thermal structure and the annual cycle, *Clim. Dyn.*, *14*, 631–644.

Pawson, S., and M. Fiorino (1998b), A comparison of reanalyses in the tropical stratosphere. Part 2: The quasi-biennial oscillation, *Clim. Dyn.*, *14*, 645–658.

Pawson, S., and M. Fiorino (1999), A comparison of reanalyses in the tropical stratosphere. Part 3: Inclusion of the pre-satellite data era, *Clim. Dyn.*, *15*, 241–250.

Plumb, R. A., and R. C. Bell (1982), A model of the quasi-biennial oscillation on an equatorial beta-plane, *Q. J. R. Meteorol. Soc.*, *108*, 335–352.

Politowicz, P. A., and M. H. Hitchman (1997), Exploring the effects of forcing quasi-biennial oscillations in a two-dimensional model, *J. Geophys. Res.*, *102*, 16,481–16,497.

Prather, M. J. (1986), Numerical advection by conservation of 2nd-order moment, *J. Geophys. Res.*, *91*, 6671–6681.

Press, W., S. Teukolsky, W. Vetterling, and B. Flannery (1992), *Numerical Recipes in Fortran 77: The Art of Scientific Computing*, 2nd ed., 933 pp., Cambridge Univ. Press, New York.

Randel, W. J., and J. B. Cobb (1994), Coherent variations of monthly mean total ozone and lower stratospheric temperature, *J. Geophys. Res.*, *99*, 5433–5447.

Randel, W. J., F. Wu, R. Swinbank, J. Nash, and A. O'Neill (1999), Global QBO circulation derived from UKMO stratospheric analyses, *J. Atmos. Sci.*, *56*, 457–474.

Randel, W. J., F. Wu, and D. J. Gaffen (2000), Interannual variability of the tropical tropopause derived from radiosonde data and NCEP reanalysis, *J. Geophys. Res.*, *105*, 15,509–15,523.

Shia, R. L., Y. L. Yung, M. Allen, R. W. Zurek, and D. Crisp (1989), Sensitivity study of advection and diffusion coefficients in a 2-dimensional stratospheric model using excess ^{14}C data, *J. Geophys. Res.*, *94*, 18,467–18,484.

Shia, R. L., Y. L. Ha, J. S. Wen, and Y. L. Yung (1990), Two-dimensional atmospheric transport and chemistry model: Numerical experiments with a new advection algorithm, *J. Geophys. Res.*, *95*, 7467–7483.

Shiotani, M. (1992), Annual, quasi-biennial, and El Niño–Southern Oscillation (ENSO) time-scale variations in equatorial total ozone, *J. Geophys. Res.*, *97*, 7625–7633.

Stevermer, A., and E. C. Weatherhead (2001), Detecting recovery in vertically-resolved ozone records, *Eos Trans. AGU*, *82*(47), Fall Meet. Suppl., F38.

Summers, M. E., D. E. Siskind, J. T. Bacmeister, R. R. Conway, S. E. Zasadil, and D. F. Strobel (1997), Seasonal variation of middle atmospheric CH_4 and H_2O with a new chemical-dynamical model, *J. Geophys. Res.*, *102*, 3503–3526.

Tung, K. K. (1984), Modeling of tracer transport in the middle atmosphere, in *Dynamics of the Middle Atmosphere*, edited by J. R. Holton and T. Matsuno, pp. 417–444, Terra Sci., Tokyo.

Tung, K. K. (1986), Nongeostrophic theory of zonally averaged circulation. Part I: Formulation, *J. Atmos. Sci.*, *43*, 2600–2618.

Tung, K. K., and H. Yang (1994a), Global QBO in circulation and ozone, Part I: Reexamination of observational evidence, *J. Atmos. Sci.*, *51*, 2699–2707.

Tung, K. K., and H. Yang (1994b), Global QBO in circulation and ozone, Part II: A simple mechanistic model, *J. Atmos. Sci.*, *51*, 2708–2721.

World Meteorological Organization (WMO) (2003), Scientific assessment of ozone depletion: 2002, *Rep. 47*, 498 pp., Global Ozone Res. and Monit. Proj., Geneva.

Yang, H., K. K. Tung, and E. Olaguer (1990), Nongeostrophic theory of zonally averaged circulation. 2. Eliassen-Palm Flux divergence and isentropic mixing coefficient, *J. Atmos. Sci.*, *47*, 215–241.

C. D. Camp, Department of Applied and Computational Mathematics, California Institute of Technology, Pasadena, CA 91125, USA. (cdc@gps.caltech.edu)

X. Jiang, Department of Environmental Science and Engineering, California Institute of Technology, Pasadena, CA 91125, USA. (xun@gps.caltech.edu)

D. Noone, R. Shia, C. Walker, and Y. L. Yung, Division of Geological and Planetary Sciences, California Institute of Technology, Mail Stop 150-21, Pasadena, CA 91125, USA. (dcn@caltech.edu; rls@gps.caltech.edu; chrisw@gps.caltech.edu; yly@gps.caltech.edu)